
Figures and figure supplements

NOVA-dependent regulation of cryptic NMD exons controls synaptic protein levels after seizure

Taesun Eom, et al.

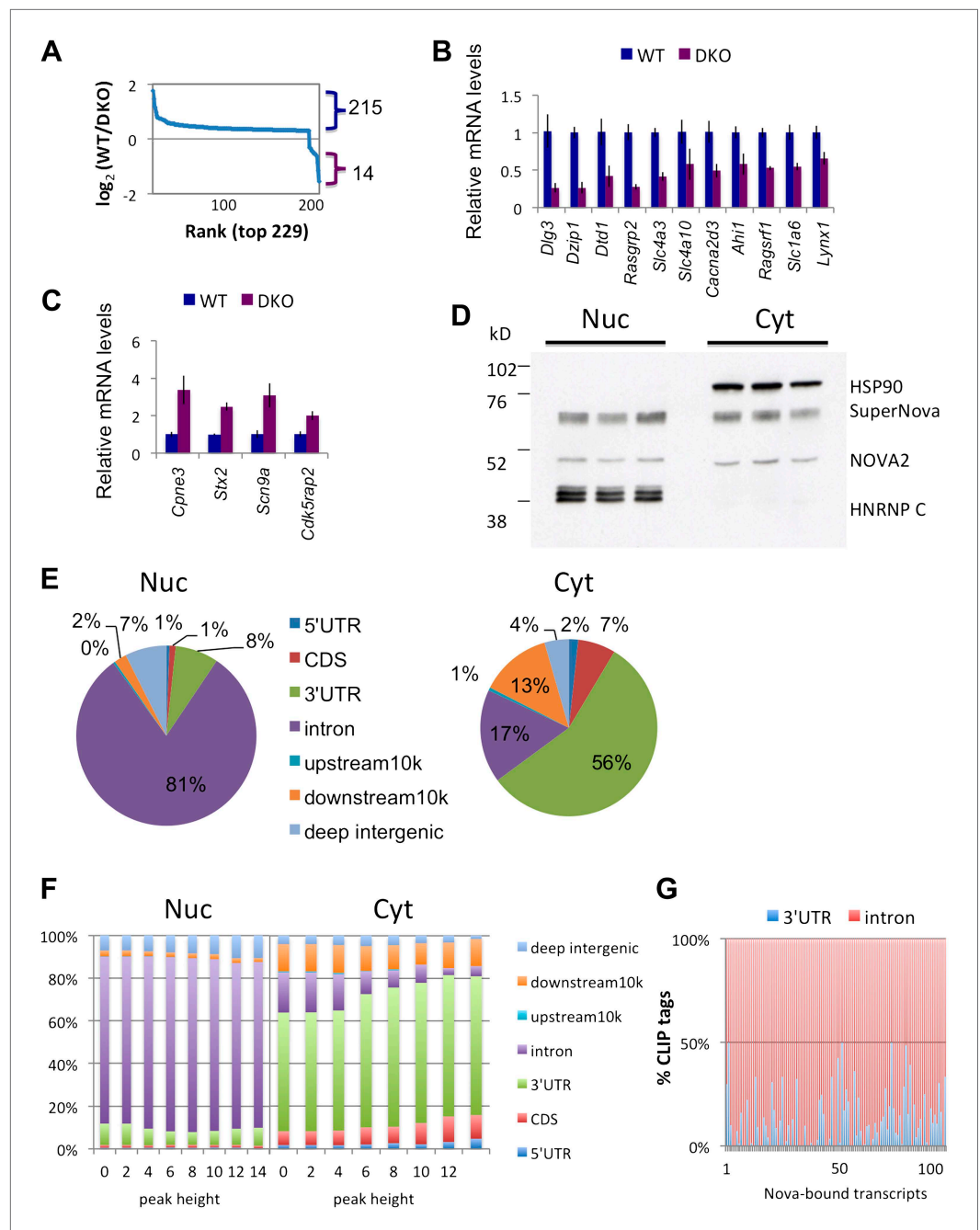


Figure 1. NOVA proteins up/down-regulate transcript levels. **(A)** Affymetrix exon arrays were interrogated with RNA from WT vs DKO E18.5 mouse whole brains, and normalized transcript intensities were plotted in \log_2 scale (\log_2 (WT/DKO) > 0.3 or < -0.3 and $p < 0.05$). The X-axis indicates ranks of transcripts from the top and Y-axis is the measure of relative transcript levels (WT/DKO) in \log_2 scale. Blue bracket represents transcripts whose levels are increased in WT relative to DKO brain (NOVA-dependent 'upregulation' of steady-state mRNA levels), and the purple bracket represents down-regulated transcripts in WT relative to DKO (NOVA-dependent repression of steady-state mRNA levels). **(B),(C)** qRT-PCR data of representative NOVA regulated transcripts. Y-axis represents the mRNA levels in which WT is normalized to 1.0. Data is from three biologic replicates (three animals) and three technical replicates (nine reactions per point); error bars represent standard deviation. For each point $p < 0.001$; see **Table 1** for additional data. NOVA up-regulated transcripts in WT versus DKO (**B**; corresponding to blue bracket in Figure 1A) and NOVA down-regulated transcripts (**C**; corresponding to purple bracket in Figure 1A) are shown. **(D)** Immunoblot analysis of NOVA distribution in nuclear and cytoplasmic fractions from mouse brain irradiated by UV. *Figure 1. Continued on next page*

Figure 1. Continued

Each lane represents the different brain extracts as biological replicates. HSP90 is used as a cytoplasmic marker, and hnRNP-C1/C2 as a nuclear marker. The NOVA2 antibody detects both large and small NOVA2 isoforms (Yang et al., 1998). (E) Breakdown of BC = 4 clusters for nuclear and cytoplasmic Nova HITS-CLIP. Downstream 10K clusters are enriched in unannotated 3' UTRs (Licatalosi et al., 2008); see also Table 2. (F) Distribution of BC = 4 clusters by peak height for both nuclear and cytoplasmic HITS-CLIP; more stringent cytoplasmic clusters show enrichment in 3' UTR. (G) Distribution of CLIP tags (intronic, red; 3' UTR, blue) from the list of NOVA up-regulated RNAs. Each point on the X-axis represents a Nova-dependent gene (in arbitrary order) and Y-axis represents the percentage of intronic/3' UTR tags for transcripts with total tags >5.

DOI: [10.7554/eLife.00178.003](https://doi.org/10.7554/eLife.00178.003)

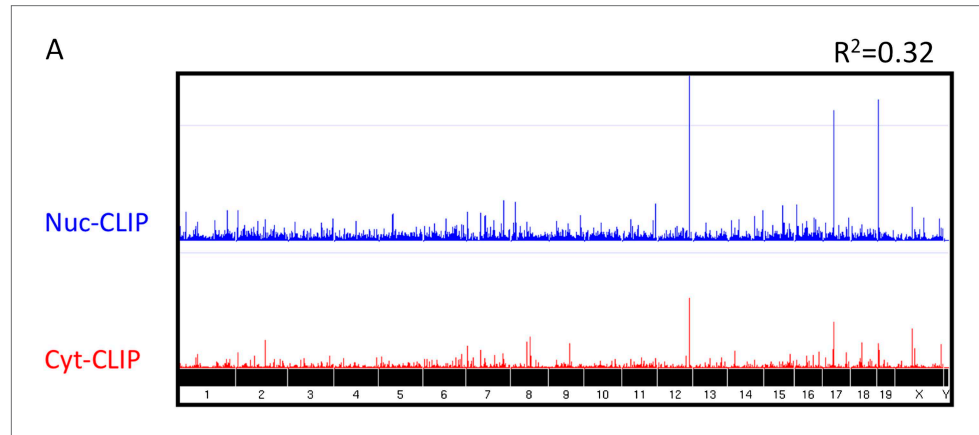


Figure 1—figure supplement 1. Nova CLIP results. Nuclear (Nuc, blue; upper) and cytoplasmic (Cyt, red; lower) HITS-CLIP tags are shown. All unique tags from nuclear and cytoplasmic HITS-CLIP clusters were plotted onto the whole genome and showed a relatively low correlation ($R^2 = 0.32$). By comparison, two independent cytoplasmic HITS-CLIP tags showed higher R^2 values (0.765; data not shown). (B) BC4 clusters were grouped according to each gene, and CLIP tags from these clusters were summed up gene-by-gene for each individual experiment, to obtain the total number of BC4 tags for each gene. The first plot (Cyt total vs Nuc total) shows the correlation ($R^2 = 0.36$) between the total number of nuclear CLIP tags per gene and the total number of cytoplasmic tags per gene; each point represents a gene. The other two plots are similar but the correlations were calculated using two Nuc CLIP experiments or two Cyt CLIP experiments.

DOI: [10.7554/eLife.00178.004](https://doi.org/10.7554/eLife.00178.004)

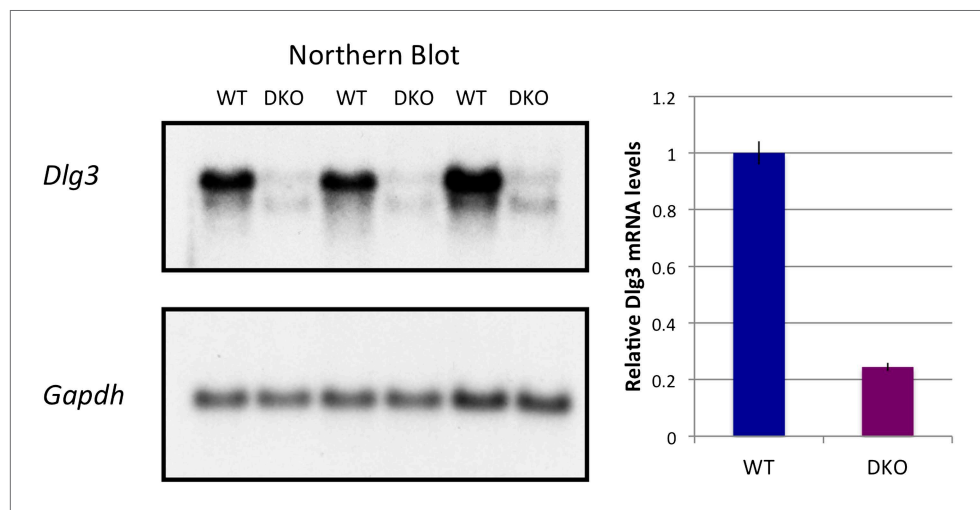


Figure 1—figure supplement 2. Correlations: analysis of Nova CLIP results. NOVA HITS-CLIP BC4 clusters were grouped according to each gene, and CLIP tags from these clusters were summed up gene-by-gene for each individual experiment, to obtain the total number of BC4 tags for each gene. The first plot (Cyt total vs Nuc total) shows the correlation ($R^2 = 0.36$) between the total number of nuclear CLIP tags per gene and the total number of cytoplasmic tags per gene; each point represents a gene. The other two plots are similar but the correlations were calculated using two Nuc CLIP experiments or two Cyt CLIP experiments.
DOI: [10.7554/eLife.00178.005](https://doi.org/10.7554/eLife.00178.005)

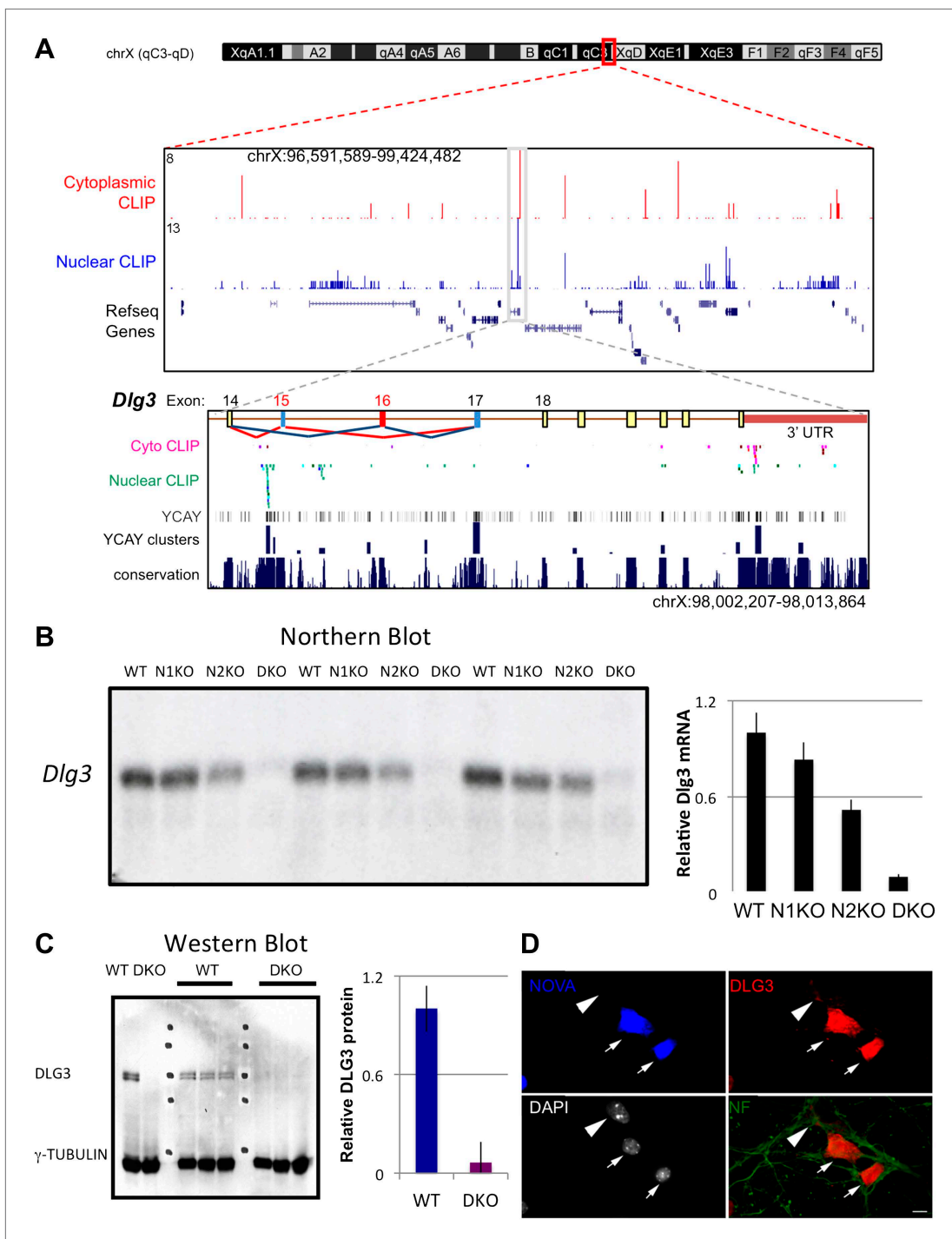


Figure 2. NOVA regulates the expression of *Dlg3* mRNA and protein. **(A)** Location of NOVA cytoplasmic and nuclear CLIP tags in chromosome X:96591589-99424482. Red and purple colors represent cytoplasmic CLIP tags and green and blue colors represent nuclear CLIP tags. The location of *Dlg3* is boxed in black and magnified in the lower box (chromosomeX:98002207-98013864). This higher magnification illustrates the position of *Dlg3* constitutive (yellow), alternative (colored) exons and 3' UTR (brown) relative to CLIP tags, YCAV elements, and sequence conservation across species. More cytoplasmic tags were evident in the 3' UTR and more nuclear tags in introns. Clusters of CLIP tags can be seen to overlap with the location of clusters of YCAV sequences (in grey) as well as bioinformatically predicated clusters of YCAV elements (in blue; see [Zhang et al., 2010](#)). **(B)** Northern blot analysis of *Dlg3* mRNA from three biologic replicates of WT or Nova KO brain mRNA. Equal amount of RNA was loaded (see [Figure 2—figure supplement 2](#)). Quantitation of relative RNA intensity (WT/DKO) was plotted as a relative ratio of *Dlg3* mRNA in WT, N1 KO, N2 KO or DKO brain as indicated; error bars represent standard deviation ($p < 0.05$); about 90% of *Dlg3* mRNA is absent in DKO brain. **(C)** Immunoblot analysis of DLG3 in [Figure 2](#). *Continued on next page*

Figure 2. Continued

WT vs DKO. Protein extracts from the four different WT or DKO mouse brains (as indicated; E18.5) were assessed, and γ -TUBULIN was used as a normalizing control. Quantitation of protein intensity is indicated in graph to the right, plotted as relative ratio of DLG3 in WT/DKO, indicate that ~90% of DLG3 protein is absent in DKO brain; error bars represent standard deviation ($p < 0.05$). (D) Immunofluorescence detection of DLG3 (red), NOVA (blue) and Neurofilament (NF) (green) proteins on WT/DKO mixed primary mouse neuronal cultures. DAPI and neurofilament stained all neuronal nuclei and processes, respectively, while NOVA staining differentiates WT and DKO neurons. The DLG3 signal was markedly reduced in DKO neurons. Scale bar: 10 μ m.
DOI: [10.7554/eLife.00178.008](https://doi.org/10.7554/eLife.00178.008)

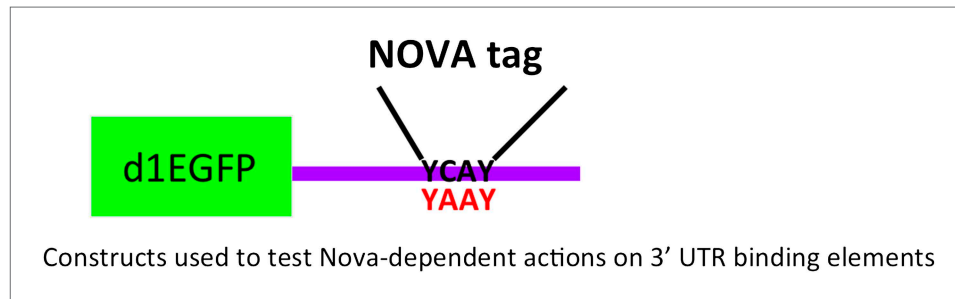


Figure 2—figure supplement 1. *Dlg3* mRNA isoforms in Nova KO brain. Northern blot analysis of *Dlg3* mRNA in WT and Nova DKO brain. (A) *Gapdh* probe was used as a normalizing control. Panel to right: Quantitation of relative RNA intensity (WT/DKO) was plotted as a relative ratio of *Dlg3* mRNA/*GAPDH* in WT/DKO; error bars represent standard deviation ($p < 0.05$). About 75% was reduced in DKO.
DOI: [10.7554/eLife.00178.009](https://doi.org/10.7554/eLife.00178.009)

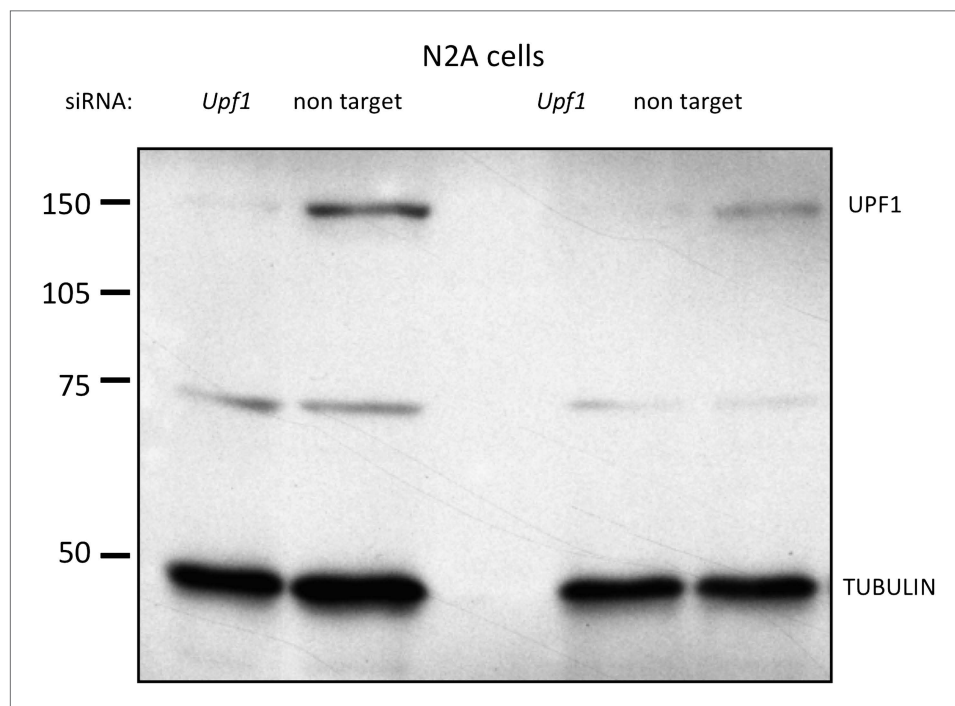


Figure 2—figure supplement 2. Northern blot analysis of *Dlg3* mRNA in Nova KO brain-reproducibility and control. Reproduction of Northern blot for *Dlg3* mRNA presented in **Figure 2B**, but also showing loading control below (Ethidium bromide (EtBr) stain of the gel), demonstrating equal loading of all RNAs.
DOI: [10.7554/eLife.00178.010](https://doi.org/10.7554/eLife.00178.010)

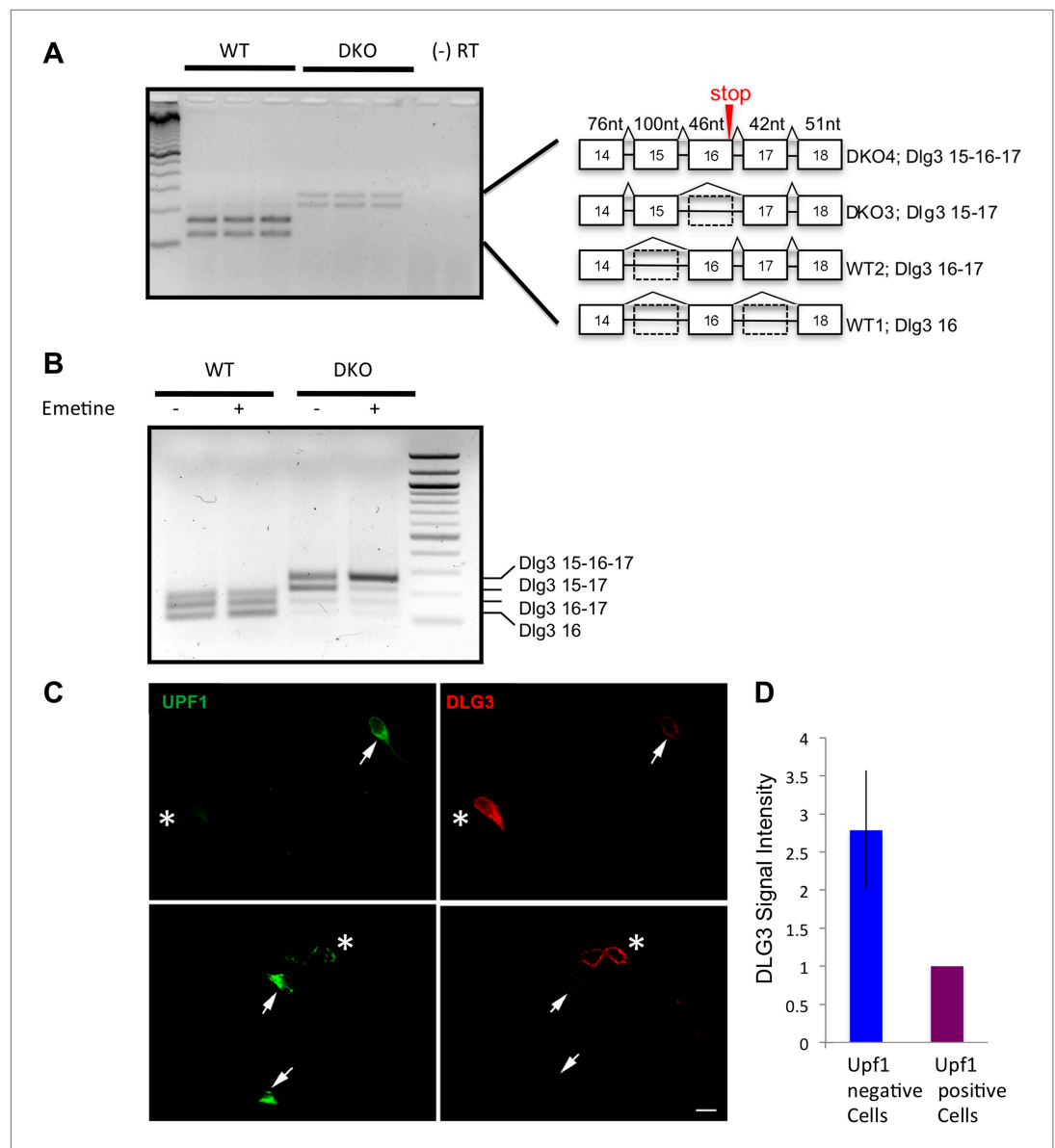


Figure 3. *Dlg3* mRNA is decreased through inclusion of cryptic NMD exons in the absence of NOVA. **(A)** RT-PCR and sequence analysis (**Figure 3—source data 1**) showed four *Dlg3* isoforms which have different combinations of alternatively spliced exons. The lower two PCR products (WT1 and WT2), respectively, harbor alternative exon 16 (E16) with or without E17, and both encode in-frame protein variants. The upper two PCR products, evident in DKO brain (DKO3 and DKO4), include E15, with or without E16, and include E17. The DKO4 isoform was not annotated in Refseq, and the combination of E15 and E16 led to a frameshift and inclusion of a premature stop codon (TAA) in E16, as indicated in the schematic (also leading us to color E16 red in **Figure 2A**). The 15–17 containing product does not make a premature stop codon. **(B)** After 6 DIV primary mouse neuronal cultures were treated with 100 $\mu\text{g}/\text{ml}$ emetine for 10 hr, RNA was harvested from triplicate samples and analyzed by RT-PCR. Emetine treatment had no effect cell viability nor on isoforms produced in WT cells, but led to accumulation of the NMD isoform DKO4 in Nova DKO neurons. Spliced isoforms are indicated. **(C)** siRNA to *Upf1* was transfected into DKO mouse primary cells, and after 24 hr, DLG3 (red) and UPF1 (green) protein was detected by immunofluorescence microscopy. Arrows indicate cells that have relatively high UPF1 levels; these cells have low DLG3 levels. In contrast, cells transfected with *Upf1* siRNA (asterisks) had markedly reduced UPF1 levels and had increased (rescued) DLG3 levels. Upper and lower rows represent independent experiments. Scale bar: 10 μm . **(D)** Quantitation of DLG3 signal in *Upf1* positive and *Upf1* knockdown cells in **(C)**. Signal intensity was normalized to the signal in *Upf1* positive cells. Error bar represents standard deviation ($p < 0.05$).

DOI: 10.7554/eLife.00178.011

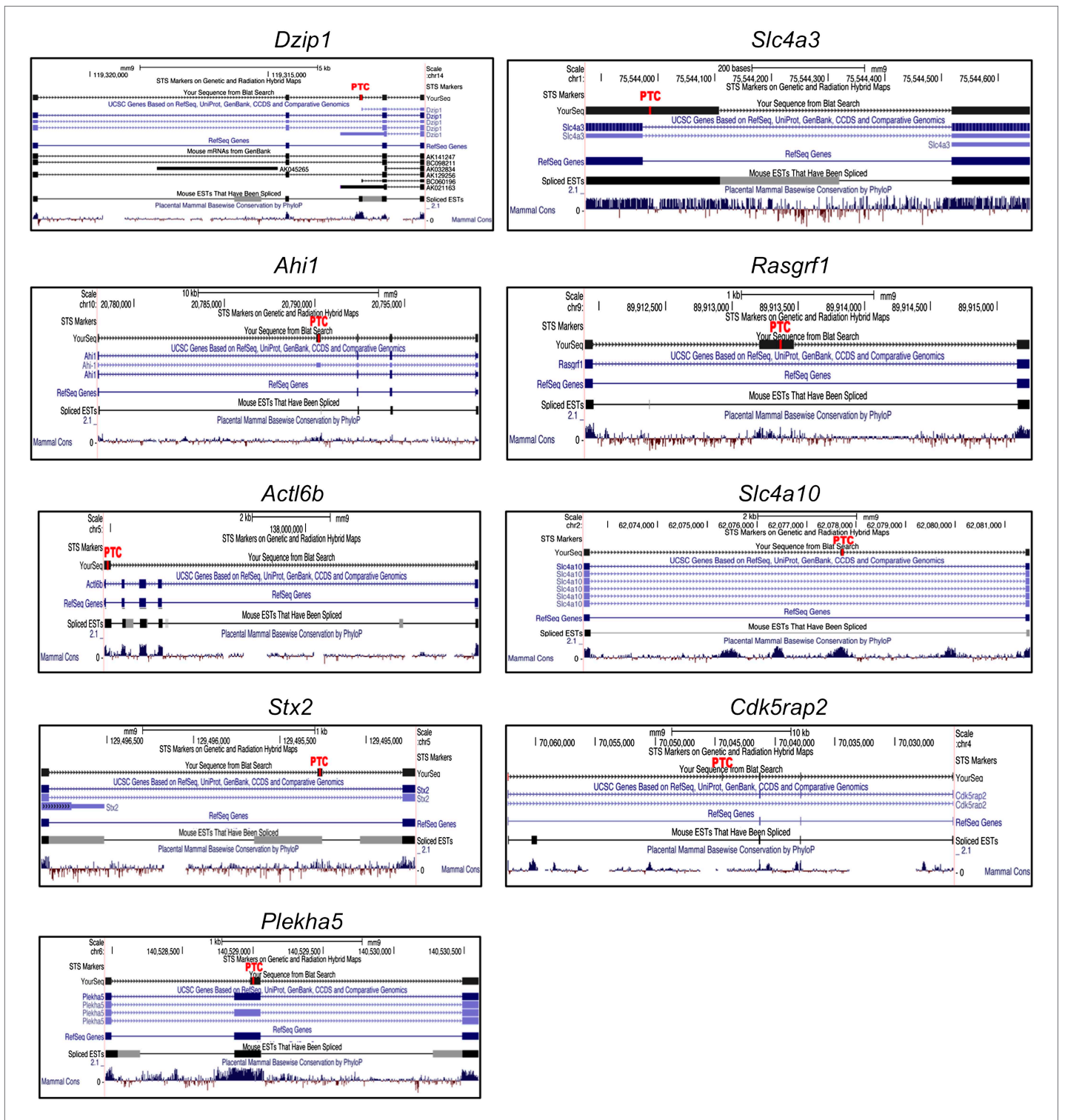


Figure 3—figure supplement 1. Reporter construct design for NOVA 3' UTR actions. Schematic of a reporter encoding destabilized d1EGFP and the 3' UTR YCAY element of NOVA's target RNA. An identical construct in which the YCAY sequences were mutated to YAAY was also made.

DOI: [10.7554/eLife.00178.013](https://doi.org/10.7554/eLife.00178.013)

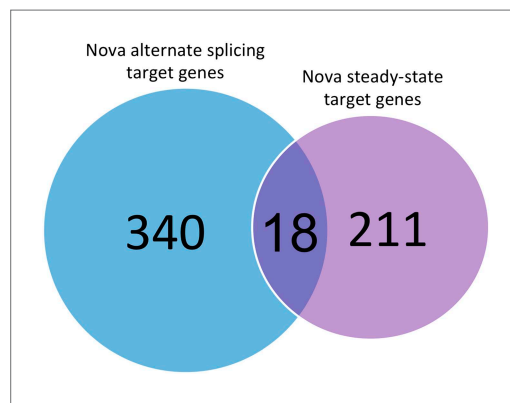


Figure 3—figure supplement 2. NOVA increases the stability of some RNAs through binding to 3' UTR YCAY elements. qRT-PCR was used to quantitate d1EGFP mRNA after transfection of various constructs (Syng3 [synaptogyrin 3], Glrb [Glycine receptor b], *Dlg3* and Syt2 [Synaptotagmin 2]). Quantitation of steady state changes in RNA levels (YAAAY relative to YCAY constructs) were 50%, 25%, 65%, 48%, respectively, for Syng3, Glrb, *Dlg3* and Syt2. The Y-axis represents the relative mRNA levels (YCAY/YAAAY). Interestingly, for *Dlg3*, a small 3' UTR construct (115 nt) did not show any change, while a longer construct (214 nt) did, even though both harbored the YCAY element, suggesting that additional elements or RNA structures may be important for binding of NOVA to this 3' UTR YCAY element. Asterisks indicate $p < 0.05$. DOI: [10.7554/eLife.00178.014](https://doi.org/10.7554/eLife.00178.014)

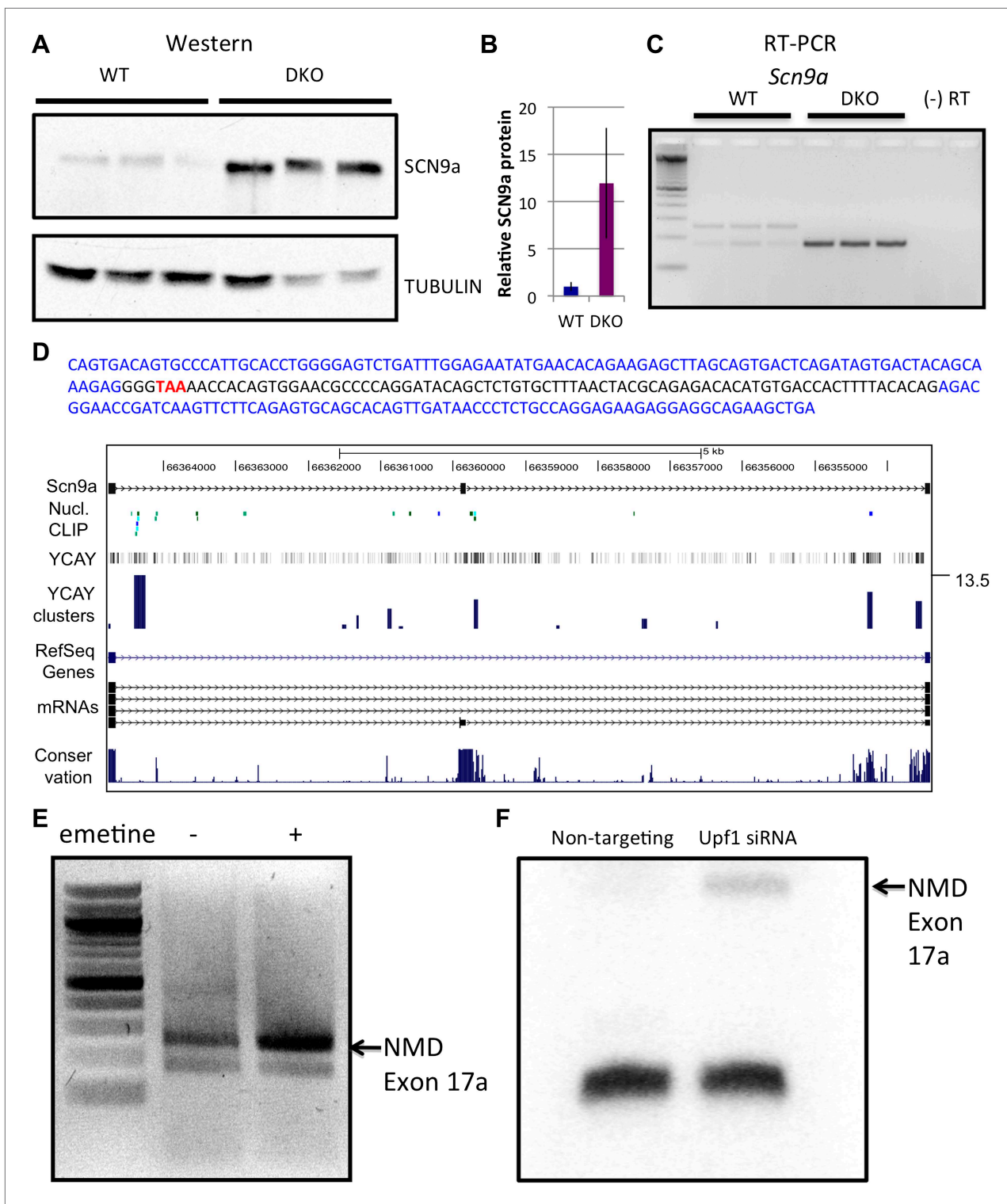


Figure 4. NOVA and NMD-mediated regulation of *Scn9a* mRNA and protein. **(A)** Immunoblot analysis of SCN9a in WT vs DKO. Proteins extracts from WT (lane 1–3) vs DKO (lane 4–6) were loaded. γ -Tubulin was used as a normalizing control. **(B)** Quantitation of relative protein intensity (WT/DKO). The results were plotted as a relative ratio of SCN9a in WT/DKO; error bars represent standard deviation ($p < 0.05$). About 90% signal was reduced in WT. **(C)** RT-PCR from WT and DKO (three biologic replicates) shows NOVA-dependent splicing of *Scn9a*. WT brains express two alternative splicing isoforms (lanes 1–3), while DKO brains express only the smaller isoform (lanes 4–6). A (-) RT control is indicated; primers are given in **Supplementary file 2**. **(D)** Sequence analysis and map of the spliced isoforms from Figure 4C showed that the larger band corresponds to a transcript in which an exon (17a) Figure 4. Continued on next page

Figure 4. Continued

was included, introducing a premature stop codon. In the sequence shown, exon 17a is highlighted in black, and the TAA premature stop codon is indicated in red. (E) Six DIV WT primary mouse neuronal cultures were treated with emetine, as indicated, for 10 hr and RT-PCR was performed. The NMD exon was increased after emetine treatment. (F) siRNA to *Upf1* or a non-targeting siRNA were transfected in WT mouse primary cells, and RT-PCR was performed with the same primers used in Figures 4C,E. The intensity of the NMD exon was increased specifically after *Upf1* siRNA treatment.

DOI: [10.7554/eLife.00178.015](https://doi.org/10.7554/eLife.00178.015)

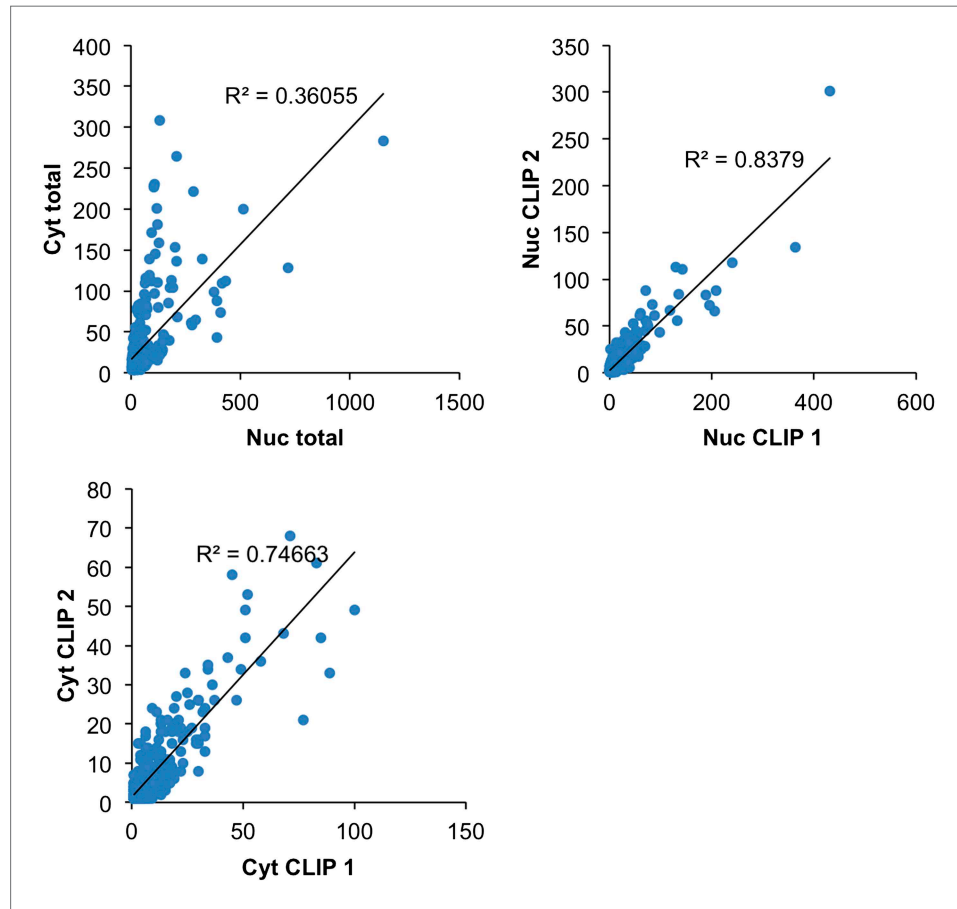


Figure 4—figure supplement 1. N2A cells: *Upf1* siRNA efficiently reduces endogenous UPF1 protein levels. siRNA targeting *Upf1* was transfected into N2a cells and immunoblot analysis of UPF1 protein was performed. Results from two independent experiments are shown. siRNA to *Upf1* showed the significant reduction of UPF1 protein expression compared with a control untargeting siRNA. γ -Tubulin was used as a normalization control.

DOI: [10.7554/eLife.00178.016](https://doi.org/10.7554/eLife.00178.016)

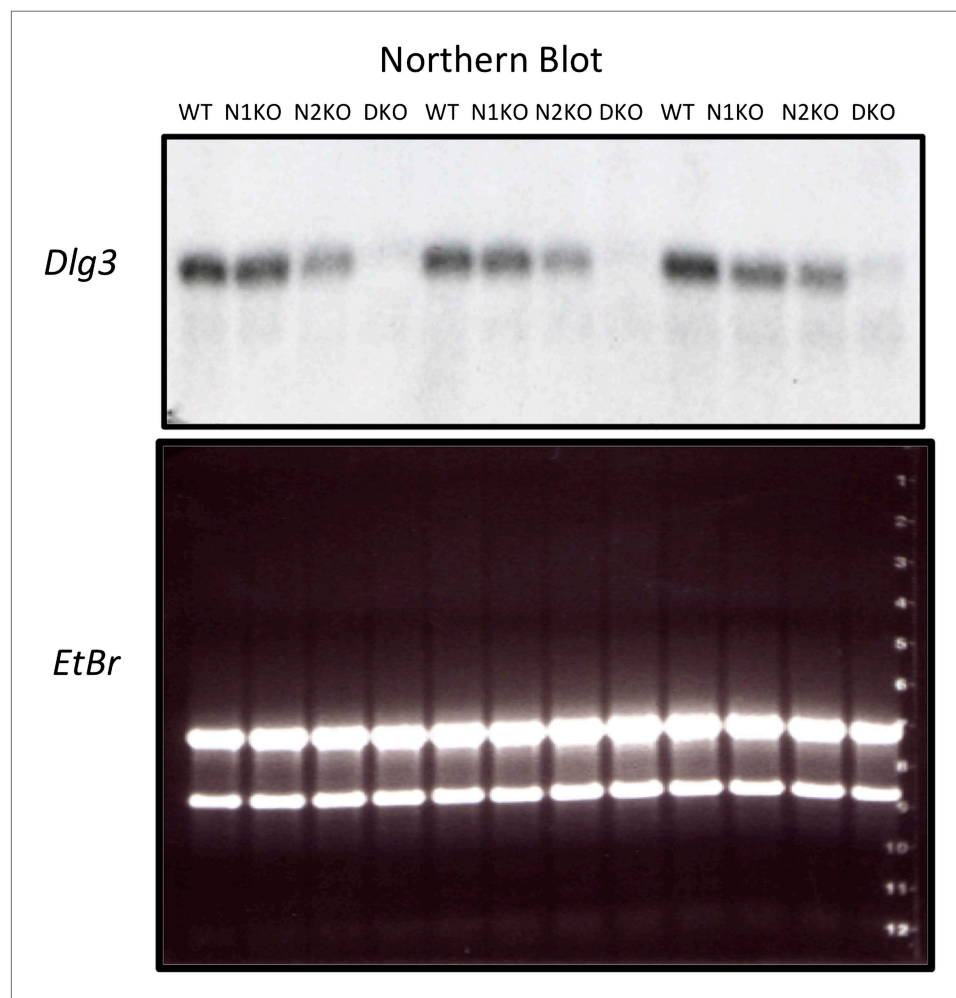


Figure 4—figure supplement 2. Primary neurons: *Upf1* siRNA reduces endogenous UPF1 protein levels. qRT-PCR quantitation of relative *Upf1* mRNA levels in primary neurons with or without treatment with *Upf1* siRNA. Error bars represents standard error of the mean; n = 3.

DOI: [10.7554/eLife.00178.017](https://doi.org/10.7554/eLife.00178.017)

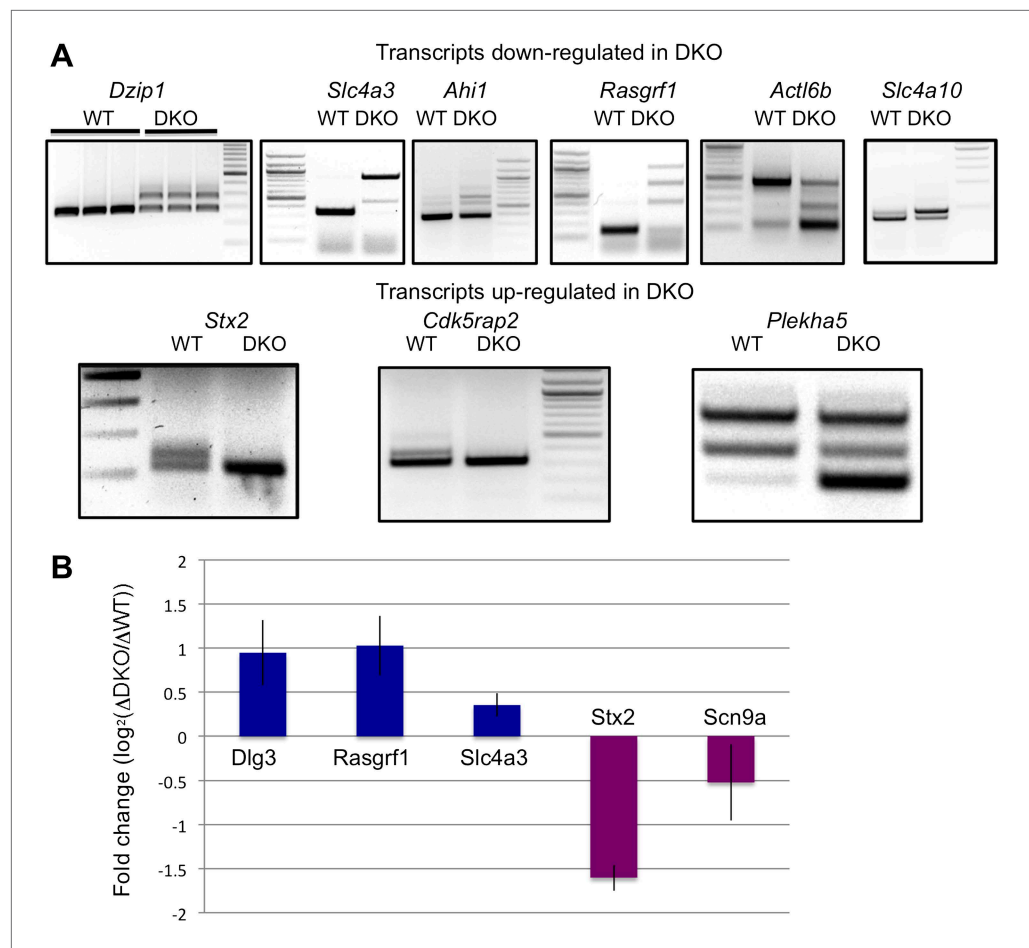


Figure 5. NOVA regulates cryptic NMD exons and transcript levels. **(A)** Analysis of alternative spliced isoforms in transcripts chosen solely on exon array data showing NOVA-dependent steady-state mRNA changes and robust HITS-CLIP clusters in introns. Transcripts were then screened for the presence of cryptic NMD exons by RT-PCR using primers in exons bounding the intronic HITS-CLIP clusters. Data is divided into those transcripts down-regulated or up-regulated in Nova DKO, as indicated. Sequence analysis of RT-PCR products showed the presence of cryptic exons harboring premature stop codons (**Figure 3—source data 1; Supplementary file 2**). A diagram of the loci of each NMD exon present in Figure 5A is shown in **Figure 5—figure supplement 1**. For example, most transcripts down-regulated in Nova DKO brains show a larger, PTC containing exon in DKO; one exception is *Actl6b*, in which in the absence of NOVA there is a PTC, and in WT brain, an upper alternate isoform (exon) is present that corrects that frame-shift; **(B)** Effect of emetine on putative NOVA-regulated cryptic NMD exons. The steady-state level of six transcripts identified in **Figures 3B, 4C and 5A** were assessed by qRT-PCR in six DIV WT vs Nova DKO primary mouse neurons incubated for 10 hr in the presence or absence of emetine. The results were plotted with the Y-axis as a measure of the degree of putative NOVA-dependent NMD regulation (the fold change of transcript levels in DKO neurons in the presence or absence of emetine, divided by that of WT, in \log_2 scale). For example, for *Dlg3* the \log_2 value is about 1.0 indicating that emetine treatment increased the *Dlg3* NMD-isoform in DKO neurons relative to WT neurons by a factor of two, while emetine decreased the NMD isoform of *Scn9a* by ~1.4-fold, leading to decrease or increase in the respective proteins in Nova DKO neurons (**Figures 2 and 3** or **Figure 4**, respectively). Three independent experiments were performed and error bars represent standard deviation ($p < 0.05$).

DOI: 10.7554/eLife.00178.018

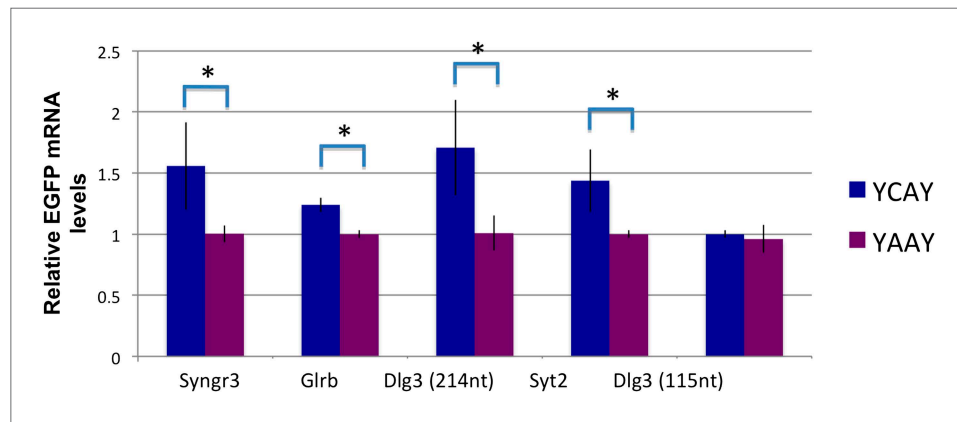


Figure 5—figure supplement 1. Diagrams of each of the NMD exons shown in **Figure 5A**. The position of the exon harboring a premature termination codon is labeled in red (PTC).

DOI: [10.7554/eLife.00178.019](https://doi.org/10.7554/eLife.00178.019)

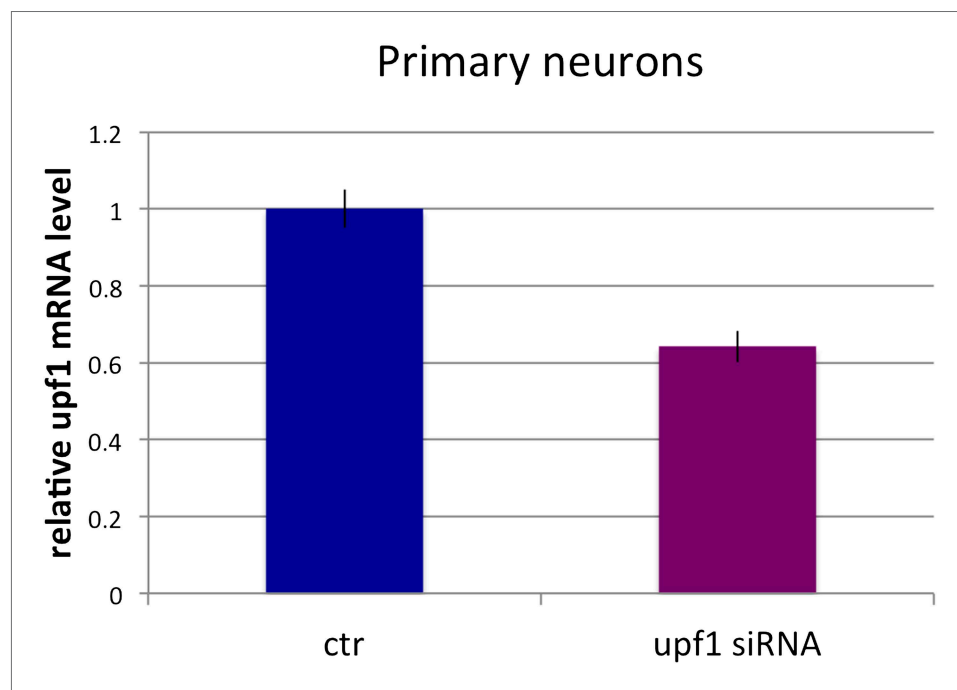


Figure 5—figure supplement 2. NOVA regulates the expression of Stx2 (Syntaxin 2) mRNA and protein. **(A)** RT-PCR from WT and DKO brain showed NOVA-dependent alternative splicing of a previously unknown, higher molecular weight isoform of Stx2. A (-) RT negative control is shown. **(B)** Immunoblot analysis of STX2 protein in biologic triplicate samples of WT vs Nova DKO brain. γ -Tubulin was used as a normalization control. **(C)** Quantitation of relative protein intensity (WT/DKO) from **(B)**, plotted as relative ratio of STX2 in WT/DKO; error bars represent standard deviation ($p < 0.05$). **(D)** Six DIV WT primary mouse culture were treated with vehicle (-) or emetine (+) for 10 hr and RT-PCR was performed for Stx2 as in **(A)**. Quantitation revealed that the NMD exon (labeled) was increased twofold after emetine treatment. **(E)** DY547 direct-labeled siRNA targeting *Upf1* was transfected into WT mouse primary cells, and immunofluorescence microscopy used to detect STX2 (green) and siRNA to *Upf1* (red). The thin arrow (top right corner) indicates a cell which was not transfected with siRNA, and which shows a baseline signal of STX2 protein. The two thicker arrows indicate cells which had a good red signal (siRNA to *Upf1*) and stronger green signals (indicating increased STX2 protein). Scale bar: 10 μ m.

DOI: [10.7554/eLife.00178.020](https://doi.org/10.7554/eLife.00178.020)

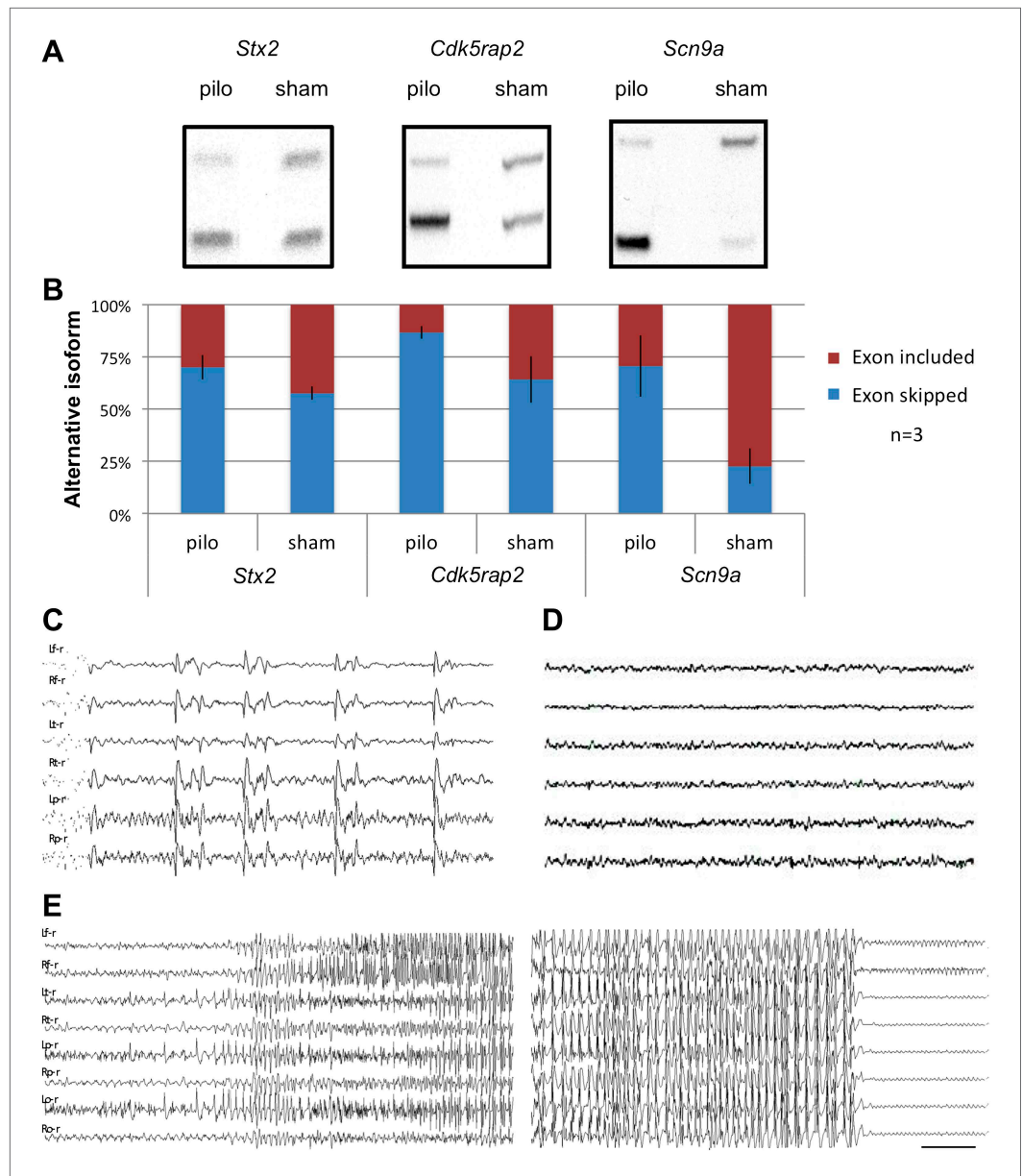


Figure 6. Seizure-induced inhibition of NOVA-regulated NMD exons. **(A)** Mice were treated with pilocarpine (pilo) to induce seizures or were mock-treated (sham). 2 hr later brains were harvested and splicing of NMD exons assayed by RT-PCR. **(B)** Quantitation of experiments described in **(A)**, from three biologic replicates. Error bars represent standard deviation ($p < 0.05$; Student's t-test). **(C),(D)** EEG of freely moving *Nova2*^{+/-} mutant displays frequent synchronous cortical interictal discharges **(C)** not detected in wild type mice **(D)**. **(E)** Spontaneous generalized seizure discharge in adult *Nova2*^{+/-} mutant. A 20 s gap of continuous hypersynchronized EEG pattern separates the beginning and end of the seizure discharge. Bilateral left and right frontal, temporal, parietal **(C, D)** and occipital **(E)** leads are shown. Time calibration 1 s **(C, D)**, 2 s **(E)**.

DOI: [10.7554/eLife.00178.021](https://doi.org/10.7554/eLife.00178.021)

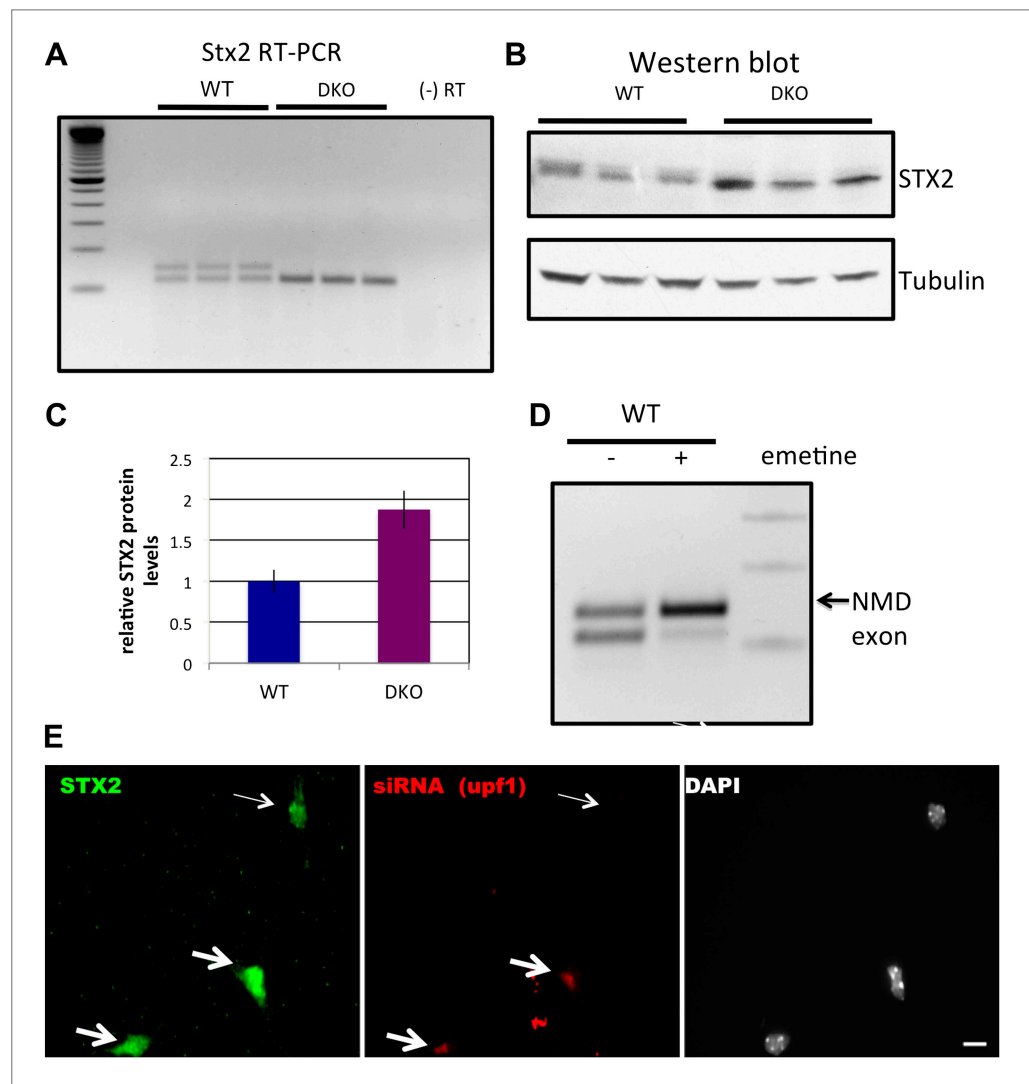


Figure 6—figure supplement 1. Comparison of different sets of transcripts regulated by NOVA. The number of transcripts in which NOVA regulates alternative splicing without changing steady-state mRNA levels are shown in blue, and in purple transcripts showing Nova-dependent changes in steady-state mRNA levels (e.g. through NMD or transcript stability). 340 transcripts in which cassette exons are regulated by NOVA were compiled from previous studies (Ule et al., 2003; Licatalosi et al., 2008; Zhang et al., 2010), and compared with the 211 transcripts identified here by exon array. The datasets are largely mutually exclusive, with only 18 transcripts in common. DOI: 10.7554/eLife.00178.022

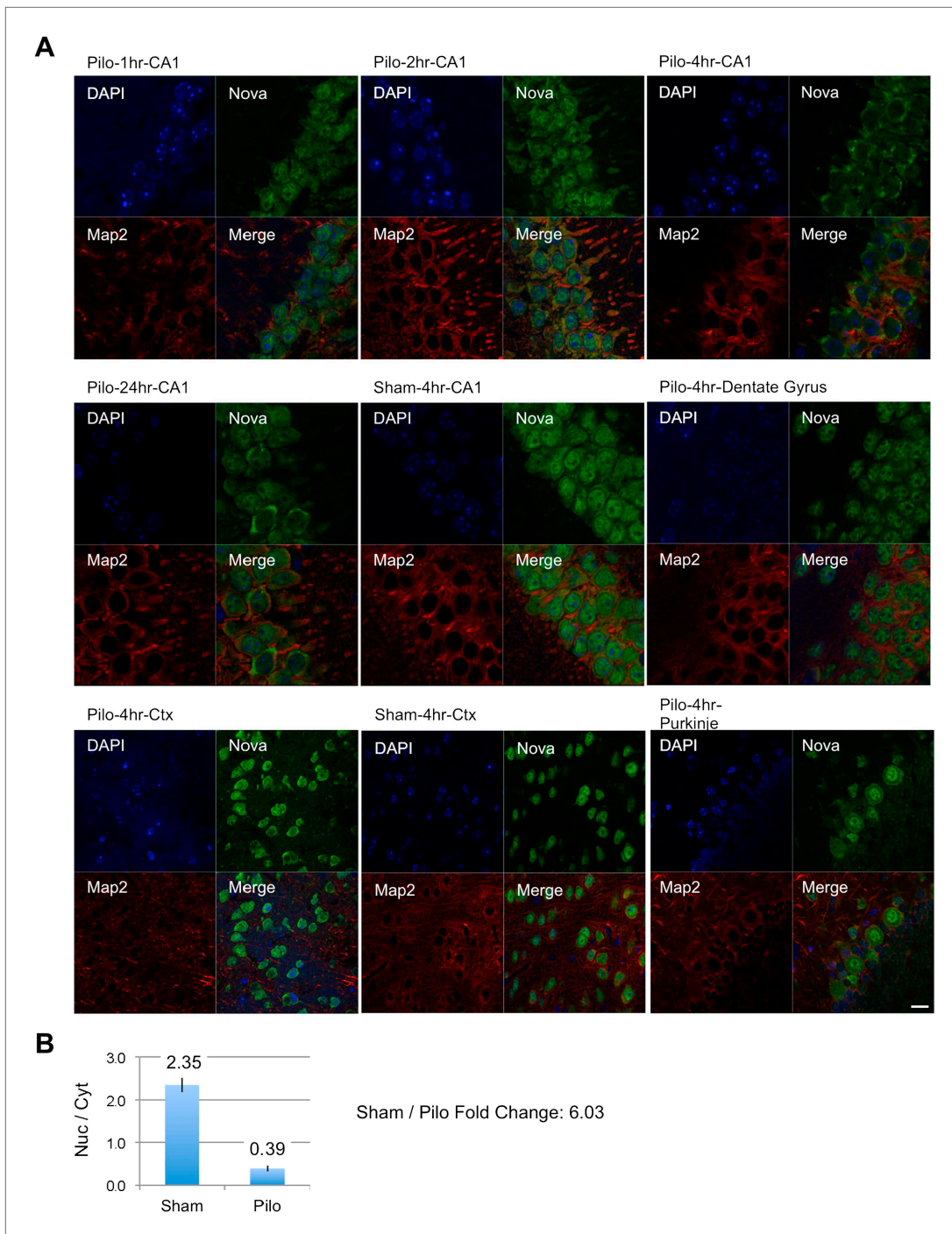


Figure 7. NOVA subcellular localization after pilocarpine-induced status epilepticus. **(A)** NOVA and MAP2 protein localization were visualized by immunofluorescence (IF) in mouse brain sections from pilocarpine treated (pilo) or control animals (sham). Regions include CA1 and dentate gyrus (DG) from hippocampal area, cortex (Ctx) and cerebellar Purkinje neurons. Changes were clearly evident in CA1 neurons, were not evident in DG, and were variable in Ctx. No changes were expected nor observed in Purkinje neurons. **(B)** Quantification of IF signal intensity from nuclear area (Nuc) divided by signal intensity from cytoplasmic area (Cyt) in CA1 neurons. Nuc/Cyt ratios (sham divided by pilocarpine signal) were obtained from 22 cells in two sham animals and 23 cells in four pilocarpine animals at the 4 hr time point. Scale bar 20 μ m.

DOI: [10.7554/eLife.00178.024](https://doi.org/10.7554/eLife.00178.024)

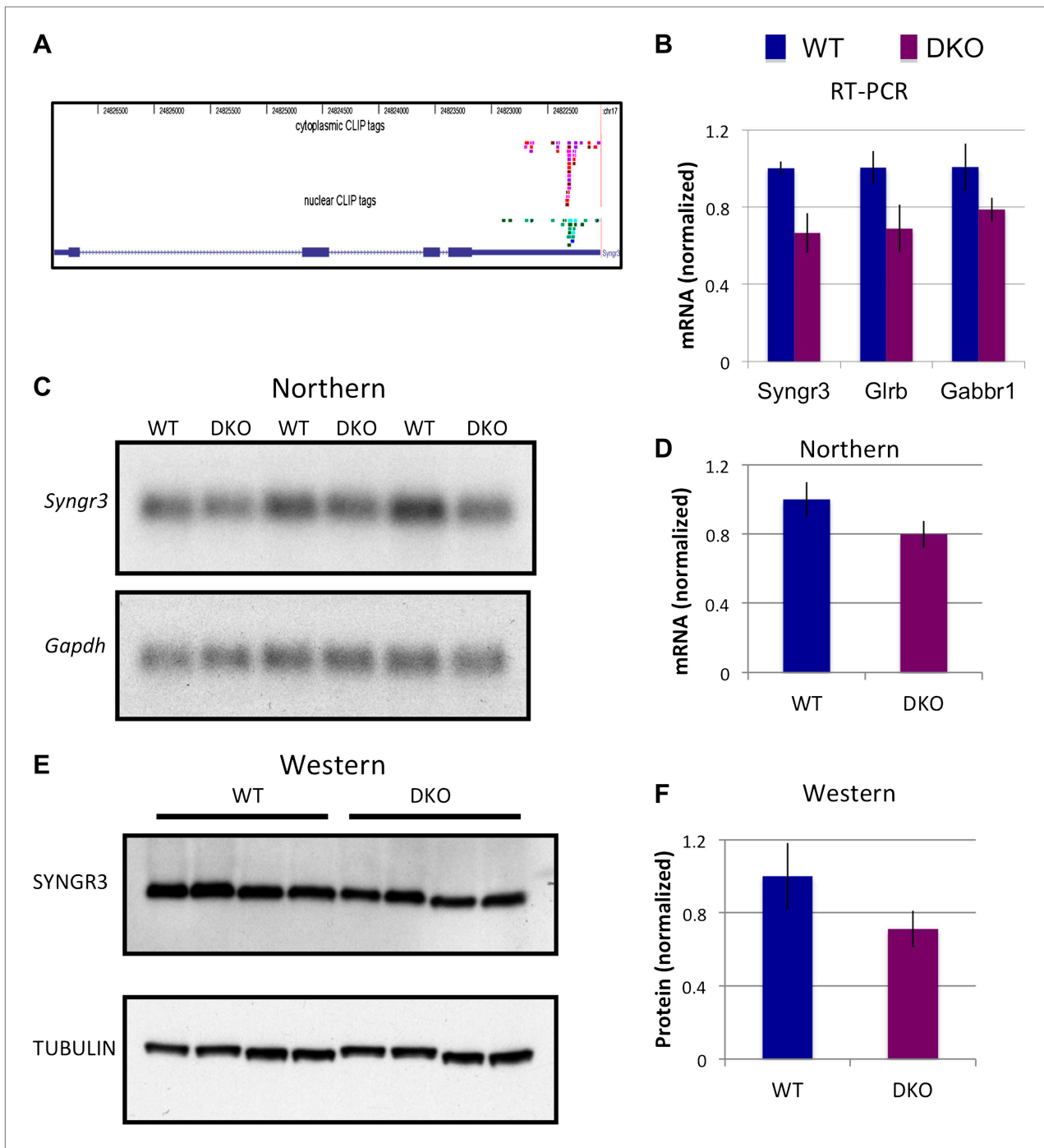


Figure 8. NOVA regulates the expression of synaptogyrin III (*Syng3*) mRNA and protein. **(A)** Location of cytoplasmic and nuclear CLIP for *Syng3*. Red and purple colors represent Cytoplasmic CLIP tags and green and blue tags represent nuclear CLIP tags. All tags were located in 3' UTR. **(B)** qRT-PCR data of *Syng3*, *Glr3* (Glycine receptor b), and *Gabbr1* (GABA B receptor1) showed mild reduction (about 30%) in *Nova* DKO brain. Y-axis represents the relative mRNA levels (WT/DKO). $p < 0.05$. **(C)** Northern blot analysis of *Syng3* mRNA in WT (lane 1, 3, 5) vs DKO (lane 2, 4, 6). *Gapdh* probe was used as a normalizing control. **(D)** Quantitation of relative RNA intensity (WT/DKO) was plotted as a relative ratio of *Syng3* mRNA/*Gapdh* in *Nova* WT/DKO; error bars represent standard deviation ($p < 0.05$); *Syng3* was reduced by about ~20% in DKO brain. **(E)** Immunoblot analysis of SYNGR3 in WT vs DKO. Protein extracts from WT (lane 1–4) vs DKO (lane 5–8) were loaded. γ -TUBULIN is used as a normalizing control. **(F)** Quantitation of relative protein intensity (WT/DKO). The results were plotted as relative ratio of SYNGR3 in WT/DKO; error bars represent standard deviation ($p < 0.05$); SYNGR3 protein was reduced ~35% in DKO brain.

DOI: 10.7554/eLife.00178.025

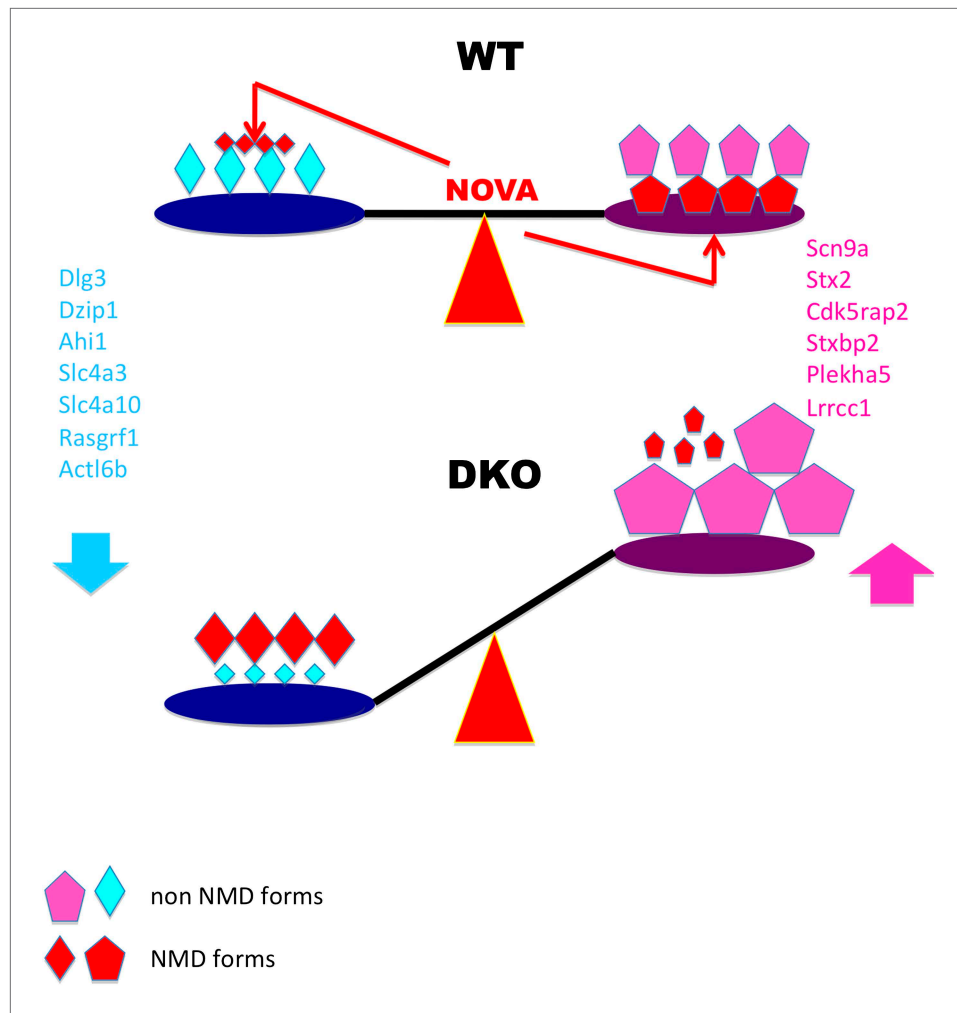


Figure 9. Model linking electrical activity with Nova-dependent splicing of cryptic NMD exons to maintain the balance of synaptic proteins. In WT brain, NOVA represses some cryptic NMD isoforms (small red diamonds on left) while promoting others (large red pentagons on right), thereby maintaining the balance of protein levels. To a lesser degree, NOVA also stabilizes transcripts through 3' UTR interactions (**Figure 8**). In DKO brain, the absence of NOVA disturbs this balance of protein in expression, contributing to aberrations in synaptic transmission. For example, Nova-regulation of cryptic NMD exons alters levels of the NMDA-receptor associated *Dlg3* (**Figures 2 and 3**) and sodium channel *Scn9a* (**Figure 4**) proteins, which are implicated in familial epileptic disorders and are dynamically regulated after seizures in mice (**Figure 6**).

DOI: [10.7554/eLife.00178.027](https://doi.org/10.7554/eLife.00178.027)